JOURNAL OF THERMOPHYSICS AND HEAT TRANSFER
Vol. 18, No. 1, January–March 2004

Low-Reynolds-Number Effects on Hypersonic Blunt-Body Shock Standoff

George R. Inger*
Iowa State University, Ames, Iowa 50011-2271

An approximate analytical theory of the onset of viscous effects on hypersonic-body nose shock standoff distance is developed. Boundary-layer displacement, shock layer vorticity, and longitudinal curvature effects are all included, as are the influence of both shock layer density ratio and arbitrary body surface temperature. Validating comparisons with both computational fluid dynamics results and experimental data are also presented.

Nomenclature

a, b, c, d	=	constants defined in Eq. (7) (Table 2)
F	=	function defined in Eq. (8)
g_w	=	T_w/T_0
j	=	0 or 1 for two-dimensional or axisymmetric flow, respectively
K	=	function defined in Eq. (4)
M	=	Mach number
Pr	=	Prandtl number
R_B	=	body nose radius (Fig. 1)
Re_{crit}	=	shock layer Reynolds number value where $(\Delta - \Delta_{\text{inv}}) = 0.10\Delta_{\text{inv}}$
Re_s	=	shock layer Reynolds number, $\rho_\infty U_\infty R_b/\mu_F$
T	=	static temperature
T_0	=	total temperature, $T_\infty\lfloor 1 + 0.5(\gamma_\infty - 1)M_\infty^2\rfloor$
U_1	=	function defined in Eq. (1)
u, v	=	x and y velocity components (Fig. 1)
x, y	=	coordinates along and normal to the body (Fig. 1)
β_{sh}	=	stagnation point velocity gradient behind shock
$\beta_{\text{sh,eff}}$	=	function defined in Eq. (5)
β_w	=	stagnation point velocity gradient on body surface
γ	=	specific heat ratio
Δ	=	shock standoff distance (Fig. 1)
δ	=	boundary-layer edge thickness
δ^*	=	boundary-layer displacement thickness
ε	=	inviscid shock layer density ratio
ζ	=	y/R_B
λ	=	parameter defined by Eq. (4)
μ	=	coefficient of viscosity
ρ	=	density

Subscripts

BL	=	boundary layer
e	=	boundary-layer edge
F	=	chemically frozen shock layer
inv	=	inviscid solution value
w	=	body surface
0	=	inviscid stagnation value
∞	=	freestream

Presented as Paper 2003-1136 at the 41st Aerospace Sciences Meeting, Reno, NV, 6–9 January 2003; received 29 January 2003; revision received 19 June 2003; accepted for publication 20 June 2003. Copyright © 2003 by the American Institute of Aeronautics and Astronautics, Inc. All rights reserved. Copies of this paper may be made for personal or internal use, on condition that the copier pay the $10.00 per-copy fee to the Copyright Clearance Center, Inc., 222 Rosewood Drive, Danvers, MA 01923; include the code 0887-8722/04 $10.00 in correspondence with the CCC.

*Professor, Department of Aerospace Engineering. Associate Fellow AIAA.

Introduction

THE standoff distance Δ of the bow shock on the nose region of a hypersonic blunt body (Fig. 1) is an important observable in experimental studies of space vehicle aerodynamics.[1] It is, therefore, useful to have an accurate, fundamentally based theory for predicting and correlating data for shock standoff over a wide range of high-altitude flight conditions. When the combination of such conditions and body size R_b involve shock layer Reynolds numbers Re_s larger than 300, viscous effects have a negligible influence on Δ, and existing inviscid methods are sufficient for the task. However, when simulating lower-Reynolds-number flight conditions corresponding to flight in rarefied atmospheric regimes, there arises the need to include the viscous effects on predictions/observations of shock standoff and to estimate under what conditions these effects can be neglected.

Exact numerical solution codes are available to serve this need; however, such purely computational fluid dynamics (CFD) tools are expensive to use for engineering parametric studies and do not readily yield the physical insight and similitude laws needed for experimental design and data interpretation. The present work offers an alternative analytical treatment yielding a closed-form prediction method that accounts for the low-Reynolds-number effects on the inviscid result and shows how such effects depend on both the shock layer density ratio and body temperature. Such a theory is useful in the design of simulation facilities for high-altitude hypervelocity flight and for the interpretation of their results.

Outline of Theory

Our main focus is on the threshold of low-Reynolds-number effects associated with the continuum end of the rarefied flow spectrum, embracing the boundary-layer/vorticity interaction shock layer regime wherein a distinct discontinuous bow shock wave still occurs. To bring out the essential viscous aspects, we assume chemically frozen shock layer conditions without dissociation; surface slip effects of velocity and temperature are also neglected. A thin constant pressure shock layer is assumed in the stagnation region of either a two-dimensional or axisymmetric hypersonic body. An arbitrary gas is treated, the body having an arbitrary temperature T_w relative to the total temperature of the flow.

A two-layered model of the shock layer is employed, consisting of an outer region of constant density vortical inviscid flow behind the shock overlaying an inner viscous sublayer adjacent to the body surface (Fig. 1). When attention is restricted to the immediate vicinity of the stagnation line where $u \approx u_1(y)\cdot x$, $\rho \approx \rho_0(y)$, and $v = v_0(y)$ (Fig. 1), the continuity equation governing the flow along this line is

$$(1 + j)\rho_0 U_1 + (1 + j)\frac{\rho_0 v_0}{R_B} + \frac{\mathrm{d}(\rho_0 v_0)}{\mathrm{d}y} = 0 \qquad (1)$$

where $j = 0$, 1 for two-dimensional and axisymmetric flows, respectively. When the integrating factor $\exp[(1 + j)y/R_B]$ is used, Eq. (1) can be integrated from the solid nonablating body surface,

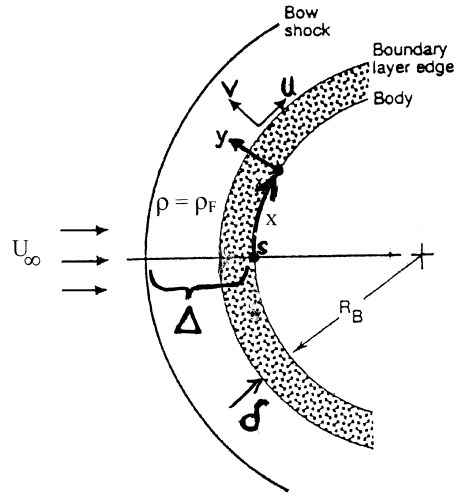

Fig. 1 Schematic of a two-layered model of the stagnation region shock layer.

$v_0 = 0$, to any distance y in the shock layer to give the mass flux there as

$$\rho_0 v_0(y) = -(1+j)\exp\left[-(1+j)\frac{y}{R_B}\right] \times \int_0^y \exp\left[(1+j)\frac{y}{R_B}\right]\rho_0 U_1\,\mathrm{d}y \tag{2}$$

Purely Inviscid Analysis

Suppose we were to neglect the inner viscous region and, thus, treat the entire shock layer as a purely inviscid flow with a constant density $\rho_0 = \rho_F \equiv \rho_\infty/\varepsilon_F$ at the limiting postshock density ratio $\varepsilon_F = (\gamma_F - 1)/(\gamma_F + 1)$ with γ_F taking values from $\frac{7}{5}$ for no vibrational excitation to $\frac{9}{7}$ for fully excited vibration. Then applying Eq. (2) to the entire shock layer with $y = \Delta_{\text{inv}}$ (the inviscid standoff distance) and using the mass conservation condition across the shock that $\rho_0 v_0(\Delta) = -\rho_\infty U_\infty$, we obtain

$$\frac{\rho_\infty U_\infty}{1+j} = \Delta_{\text{inv}} \int_0^1 \exp\left[-(1+j)\frac{\Delta}{R_B}(1-\zeta)\right]\rho_0 U_{1,\text{inv}}(\zeta)\,\mathrm{d}\zeta \tag{3}$$

where $\zeta \equiv y/\Delta$. Now, for thin hypersonic stagnation shock layers, the approximation $U_{1,\text{inv}} \approx \beta_{\text{sh}}$ (the stagnation point velocity gradient right behind the shock) is an accurate one. Furthermore, because Δ/R_B in the integrand is small compared to one, the exponential term can be approximated by a linear function and the resulting integral evaluated on the basis of a thin shock layer value for Δ/R_B therein; then

$$\frac{\Delta_{\text{inv}}}{R_B} \cong \frac{(1+\lambda)\varepsilon_F}{(1+j))K(\beta_w R_B/U_\infty)} \tag{4}$$

where $\lambda \equiv 1/2\varepsilon_F/(\beta_w R_B/U_\infty K)$ is a longitudinal curvature parameter and $K \equiv \beta_{\text{sh}}/\beta_w$ is the ratio of the postshock to body inviscid velocity gradients and, hence, reflects the inviscid shock layer vorticity. According to Newtonian theory (see Ref. 2), $\beta_W R_B/U_\infty \approx \sqrt{[2\varepsilon_F(1-\varepsilon_F)]}$, and values of K and λ obtained from Ref. 2 are given in Table 1 as a function of the shock layer density ratio $\varepsilon_F \equiv \rho_\infty/\rho_F$. With a value for γ_F assumed and, hence, the limiting shock layer density ratio ε_F (described earlier), Eq. (4) enables a calculation of Δ_{inv}/R_B using the aforementioned Newtonian expression for β_w and Table 1. For example, taking $\gamma_F = \frac{7}{5}(\varepsilon_F = \frac{1}{6})$ yields the value $\Delta_{\text{inv}}/R_B = 0.142$, which is in reasonably good agreement with both Hornung's[3] experimental value 0.137 obtained for nitrogen and the hypersonic limit value 0.140 indicated by the air data correlation of Ambrosio and Wortman.[4] Predictions from Eq. (4) are also in excellent agreement with both exact CFD-type calculations and experimental measurements on hypersonic cylinders and spheres at high Reynolds numbers when nonequilibrium chemistry effects are negligible.[5]

Table 1 Vortical shock layer properties vs density ratio (from Ref. 2)

		Cylinder, $j=0$		Sphere, $j=1$	
ε_F	λ	K	F	K	F
0.250	0.204	1.053	0.607	1.112	0.406
0.200	0.177	1.095	0.543	1.185	0.355
0.167	0.158	1.135	0.496	1.250	0.318
0.143	0.144	1.170	0.459	1.309	0.290
0.125	0.134	1.204	0.429	1.367	0.267
0.111	0.125	1.234	0.405	1.419	0.249
0.100	0.118	1.263	0.384	1.467	0.234
0.083	0.106	1.314	0.351	1.560	0.209
0.067	0.095	1.384	0.315	1.685	0.183
0.050	0.081	1.486	0.271	1.870	0.152
0.010	0.036	2.333	0.114	3.568	0.053

Two-Layered Analysis Including Viscosity

We now include the presence of an inner region of thickness δ that contains viscous effects in the form of a boundary-layer-type of behavior. Returning to Eq. (2) and subdividing the integration into viscous and (outer) inviscid region contributions, we have at the true shock location $y = \Delta$:

$$\rho_\infty U_\infty = (1+j)\int_0^\delta \exp\left[-(1+j)\frac{\delta - y}{R_B}\right](\rho_1 U_1)_{\text{BL}}\,\mathrm{d}y + (1+j)\rho_F\beta_{\text{sh}_{\text{eff}}}\left\{\Delta\int_0^1 \exp\left[-(1+j)(1-\zeta)\frac{\Delta}{R_B}\right]\mathrm{d}\zeta - \delta\int_0^1 \exp\left[-(1+j)(1-\zeta')\frac{\delta}{R_B}\right]\mathrm{d}\zeta'\right\} \tag{5}$$

where $\zeta' \equiv y/\delta$ and $\beta_{\text{sh,eff}}$ is the effective postshock velocity gradient that now includes the viscous displacement effect on the inviscid tangential velocity field. Under the thin constant density shock layer conditions considered here, Eq. (5) may be further simplified as described in the Appendix, with the final resulting equation indicating the explicit effects of viscosity on standoff relative to the purely inviscid theory value, namely,

$$\frac{\Delta}{R_B} \cong \frac{\Delta_{\text{inv}}}{R_B} + \frac{\delta^*}{R_B} + (1+\lambda)\underbrace{\left(\frac{K-1}{K}\right)\left(\frac{\delta - \delta^+}{R_B}\right)}_{\text{vorticity}} + \left(\underbrace{\lambda}_{\substack{\text{displacement}\\ \text{speed}}} + \underbrace{\frac{\Delta_{\text{inv}}}{R_B}}_{\text{curvature}}\right)\frac{\delta^*}{R_B} \tag{6}$$

This relationship clearly brings out that the relative viscous effect on the inviscidly predicted shock standoff is not only due to the direct effect of the boundary-layer displacement but is also composed of contributions from the vorticity in the outer layer (which is the dominant one), the longitudinal curvature, and the displacement influence on the inviscid flow speed. Because δ^* is negative for cooled bodies, whereas the value of $\Delta - \Delta_{\text{inv}}$ at lower Reynolds numbers is known to be greater than zero, the naïve use of the intuitive estimate $\Delta \cong \Delta_{\text{inv}} + \delta^*$ is seen from Eq. (6) to give an unsatisfactory result.

The explicit dependence of the foregoing on Reynolds number and wall temperature can now be revealed by supplying values of δ and δ^* as given by classical stagnation point boundary-layer theory. Neglecting second-order wall velocity and temperature slip effects, which have been shown to be very small compared to that of vorticity,[6] we can obtain these values from Emanuel's[7]

Table 2 Parameters in the shock standoff theory, Eq. (8) (based on Ref. 7)

	Cylinder, $j=0$				Sphere, $j=1$			
Pr	a	b	c	d	a	b	c	d
0.725	−0.304	0.902	2.220	0.480	−0.256	1.024	2.319	0.804
1.000	−0.158	0.806	1.956	0.423	−0.109	0.914	2.043	0.708

comprehensive numerical study of self-similar boundary-layer properties, which for stagnation flow can be rendered in the following very convenient format displaying the Reynolds number and wall temperature effects:

$$\delta^* \Big/ R_B = \sqrt{\varepsilon_F/(1+j)(\beta_w R_B/U_\infty)Re_s}(a+bg_w) \qquad (7a)$$

$$\delta/R_B = \sqrt{\varepsilon_F/(1+j)(\beta_w R_B/U_\infty)Re_s}(c+dg_w) \qquad (7b)$$

where the constants a, b, c, and d depend only on the Prandtl number and body dimensionality as given in Table 2. Incorporation of Eq. (7) into Eq. (6), thus, produces the final working form of our closed-form analytical solution:

$$[(\Delta-\Delta_{\text{inv}})/R_B]Re_s^{\frac{1}{2}} = (1+\lambda)F(j,\varepsilon_F) \times (\{1+[2\lambda/(1+j)]\}(a+bg_w)+(k-1)(c+dg_w)) \qquad (8)$$

where $F(j,\varepsilon_F) \equiv K^{-1}\sqrt{[\varepsilon_F/(1+j)(\beta_w R_B/U_\infty)]}$ is tabulated for convenience in Table 1.

Comparisons with Numerical Solutions and Experiment

First note that the breakdown into various contributions shown in Eq. (6) is consistent with the classification of low-Reynolds-number effects in hypersonic blunt-nose regions given some time ago by Van Dyke.[8] Second, the present analytical predictions that $\Delta-\Delta_{\text{inv}}$ increases with reducing Reynolds number Re_s in a manner scaling with Reynolds number $Re_s^{-1/2}$ and that this increase be considerable larger in the two-dimensional case, $j=0$, than in the axisymmetric case, $j=1$ are both in qualitative agreement with the results given by Probstein and Kemp[9] based on numerical solutions of the complete viscous shock layer equations (Fig. 2). The present theory is in excellent quantitative agreement as well for the case of the sphere; in this case, it shows that a hundred-fold reduction in Reynolds number Re_s yields a 33% increase in the shock standoff distance. The initial departures from the inviscid shock standoff value are due to the significant vorticity interaction effect in the outer part of the shock layer right behind the shock, an effect that is known to be larger in the three-dimensional case than in the two-dimensional case. The accuracy of our theory for the cylinder would, thus, be expected to be less than for the sphere; although still within 10% of the exact solution, this is indeed seen to be the case in Fig. 2.

To compare results with available experimental data, Fig. 3 shows a comparison of the present theoretical predictions of the low-Reynolds-number effect along with data obtained at Arnold Engineering and Development Center[10] for the case of a cool ($g_w \approx 0.30$) sphere in argon at several different high freestream Mach numbers. When it is considered that our theory is a strongly hypersonic one, its predictions of an increase in standoff distance with decreasing Reynolds number are seen to be in good agreement with these data. Further confirmation of our theory may be observed in Fig. 4, where its prediction of increasing Δ/R_B with decreasing Reynolds number Re_s in the higher-Reynolds-number regime is seen to be in good agreement with the collective results of various other Navier–Stokes CFD solutions correlated in Ref. 11. As expected, the present theory clearly breaks down when $Re_s \leq 200$, when fully viscous/nonadiabatic shock layer conditions obtain throughout the entire shock layer.

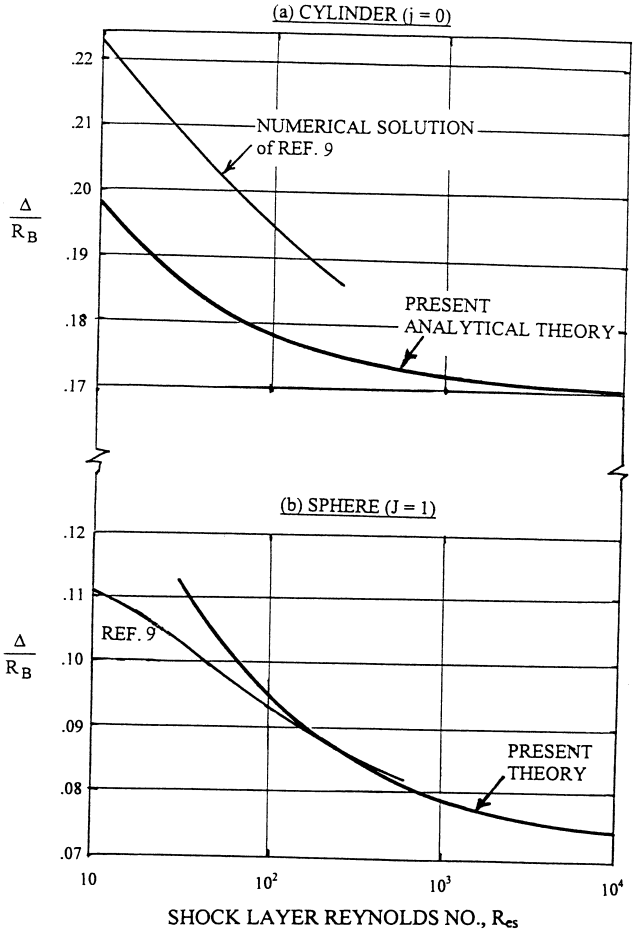

Fig. 2 Comparison of shock standoff distance predictions for highly cooled bodies ($g_w \to 0$)$\varepsilon_F = 0.11$.

Parametric Studies

The aforementioned validating comparisons and the analytical nature of our results make the present theory attractive for some instructive parametric studies. In particular, it permits direct examination of the role of both wall temperature and shock layer density ratio effects on the low-Reynolds-number behavior of shock standoff: These are shown in Fig. 5.

Figure 5 shows, first, that for a given dimensionality and ε_F cooling the body dramatically reduces Δ; indeed, this is evident by direct inspection of Eq. (8). Second, it is seen that this influence of cooling depends significantly on the shock layer density ratio being appreciably larger at higher values of ε_F. (Conversely, note that the influence of density ratio in decreasing Δ on a cooled wall is reversed when the wall is at nearly adiabatic conditions.) Finally, note from Fig. 4 that the cooling effect in the two-dimensional case can produce significantly negative values of $\Delta-\Delta_{\text{inv}}$, that is, a reduction with decreasing Reynolds number Re_s, due to the larger displacement thickness effect relative to vorticity compared to the three-dimensional case.

It has been suggested by several of the author's experimental colleagues that it might be useful to display the forgoing results as the ratio of $\Delta-\Delta_{\text{inv}}$ to the corresponding boundary-layer

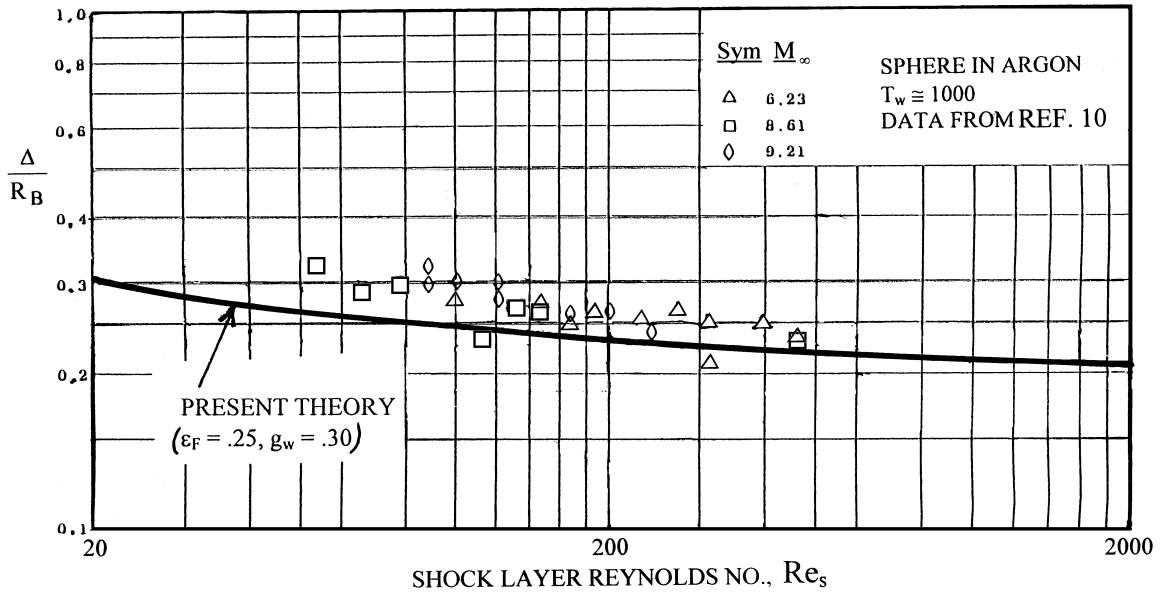

Fig. 3 Comparison of present theory with experiment.

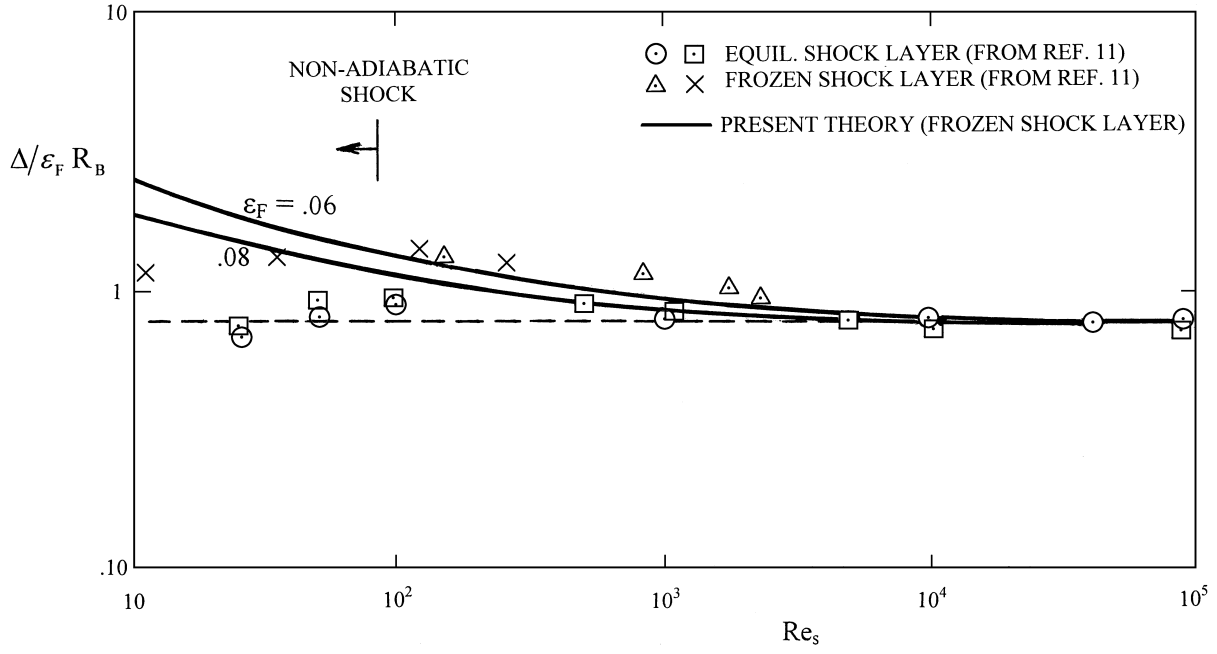

Fig. 4 Comparison of present theory with various CFD solutions.

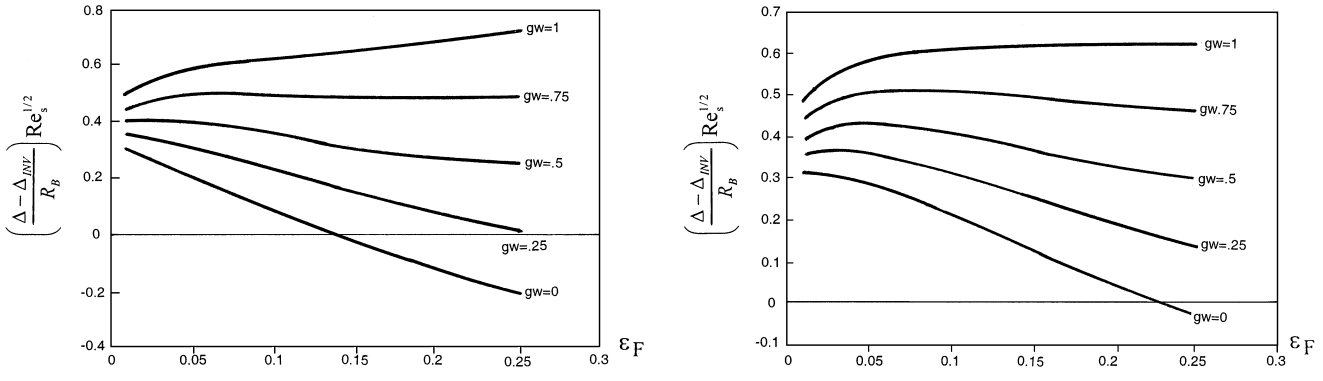

a) $j = 0$ b) $j = 1$

Fig. 5 Density ratio and wall temperature effects on scaled standoff distance.

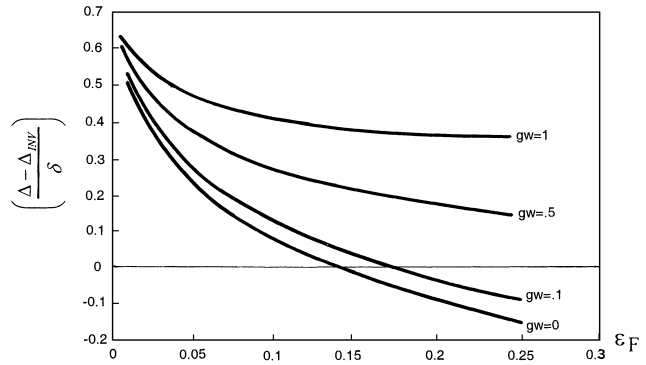

a) $j = 0$

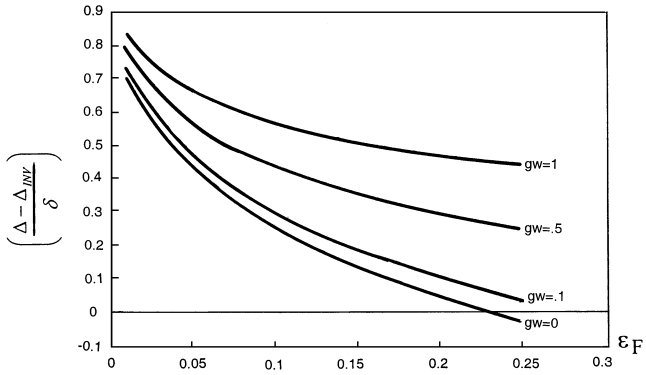

b) $j = 1$

Fig. 6 Boundary-layer thickness: scaled standoff distance vs ε_F and g_w.

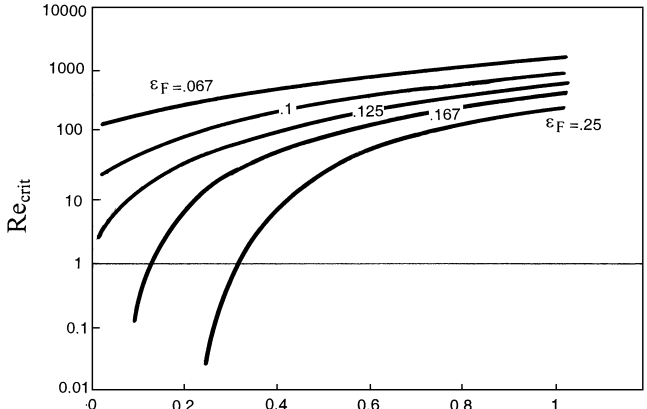

a) $j = 0$

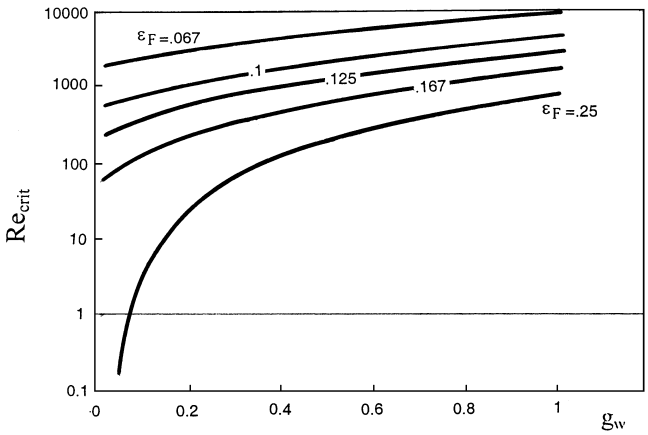

b) $j = 1$

Fig. 7 Critical Reynolds number for significant viscous effect on shock standoff.

thickness δ; accordingly, this is presented in Fig. 6. In all cases, it is seen from Fig. 6 that the low-Reynolds-number effect on standoff is less than a boundary-layer thickness, indeed it is but a small fraction thereof when the wall is highly cooled at density ratios of 0.1 or more.

Another practical feature that can be extracted from the present theory is the Reynolds number Re_{crit} at which the predicted increase in $\Delta - \Delta_{\text{inv}}$ exceeds, for example, 10% of the inviscid value: This is presented in Fig. 7 as a function of both ε_F and g_w for either two-dimensional or axisymmetric bodies. It is seen that Reynolds number Re_{crit} is reduced significantly below 10^3 by surface cooling when $\varepsilon_F > 0.10$, especially in the two-dimensional case. These trends are consistent with theoretical and experimental observations regarding the companion low-Reynolds-number effect on stagnation heat transfer.[12]

Conclusions

In the absence of significant shock layer nonequilibrium dissociation or ionization, the present theory offers a convenient analytical tool which both illuminates the dominant physics of the low Reynolds effect on blunt-body shock standoff and provides a method for estimating this effect in practical free-flight or ground-based hypervelocity simulation facilities. Given the complexities of nonequilibrium diffusion and reaction in the boundary layer, the extension of the present work to nonequilibrium shock layer flow conditions would prove formidable.

Appendix: Derivation of Equation (6)

We simplify Eq. (5) by implementing the following steps: First, the thin shock layer approximation is applied to the integrands of the second and third terms on the right by using a linear approximation to the exponential terms. After evaluating the resulting integrals and dividing the resulting equation through by $(1 + j)\beta_{\text{sh,eff}}\rho_F R_B/(1 + \lambda)$, we obtain the relationship

$$\frac{(1+\lambda)\varepsilon_F U_\infty/R_B}{(1+j)\beta_{\text{sh,eff}}} \cong \frac{\Delta}{R_B} - \left[\frac{(1+\lambda)}{1+(\delta/\Delta)}\lambda\right]\frac{\delta}{R_B}$$

$$- \frac{(1+\lambda)\beta_w}{\beta_{\text{sh,eff}}}\int_0^\delta \exp\left[-(1+j)\frac{\delta-\gamma}{R_B}\right]\left(\frac{\rho U}{\rho_e u_e}\right)_{\text{BL}} \mathrm{d}y \quad \text{(A1)}$$

where we have written $(\rho_1 U_1)_{\text{BL}} = (\rho U/\rho_e U_e)_{\text{BL}} \cdot \beta_w \rho_F$ near the stagnation point. Second, because our goal is a first-order account of the viscous effects on Δ, we can neglect the contributions of $\delta\lambda/\Delta$ and $(1 + j)(\delta - y)/R_B$ (which are second order) to the coefficients of the second and third viscous terms on the right, respectively. Third, to the same order of approximation, we take $\beta_{\text{sh,eff}} \cong K\beta_w[R_B/(R_B + \delta^*)] \cong K\beta_w[1 - (\delta^*/R_B)]$, where δ^* is the first-order boundary displacement thickness. Then noting that by definition

$$\int_0^\delta \left(\frac{\rho U}{\rho_e U_e}\right)_{\text{BL}} \mathrm{d}y \equiv \delta - \delta^*$$

the aforementioned steps and some rearrangement produce Eq. (6) from Eq. (A1).

References

[1]Morgan, R. G., "A Review of the Use of Expansion Tubes for Creating Superorbital Flows," AIAA Paper 97-0279, 1997.

[2]Hayes, W. D., and Probstein, R. F., *Hypersonic Flow Theory*, Academic Press, New York, 1959, pp. 150–162.

[3]Hornung, H. G., "Non-Equilibrium Dissociating Nitrogen Flow over Spheres and Circular Cylinders," *Journal of Fluid Mechanics*, Vol. 53, 1972, pp. 149–176.

[4]Ambrosio, A., and Wortman, A., "Stagnation Point Shock Detachment Distance for Flow Around Spheres and Cylinders," *American Rocket Society Journal*, Vol. 32, No. 2, 1962, p. 281.

[5]Inger, G. R., Higgins, C., and Morgan, R., "Shock Standoff on Hypersonic Blunt Bodies in Nonequilibrium Gas Flows," *Journal of Thermophysics and Heat Transfer*, Vol. 16, No. 2, 2002, pp. 245–250.

[6]Maslen, S. M., "Second-Order Effects in Laminar Boundary Layers," *AIAA Journal*, Vol. 1, No. 1, 1963, pp. 33–40.

[7]Emanuel, G., *Analytical Fluid Dynamics*, Chemical Rubber Press, Boca Raton, FL, 1994, pp. 265–272.

[8]Van Dyke, M., "Second Order Compressible Boundary Layer Theory with Application to Blunt Bodies in Hypersonic Flow," *Hypersonic Flow Research*, edited by F. R. Riddell, Academic Press, New York, 1962, pp. 37–76.

[9]Probstein, R. F., and Kemp, N. M., "Viscous Aerodynamic Characteristics in Hypersonic Rarefied Flow," *Journal of the Aeronautical Sciences*, Vol. 27, No. 3, 1960, pp. 174–192.

[10]Bailey, A. B., and Sims, W. H., "Shock Detachment Distance for Blunt Bodies in Argon at Low Reynolds Number," *AIAA Journal*, Vol. 1, No. 12, 1963, pp. 2867, 2868.

[11]Inger, G. R., "Non-Equilibrium Hypersonic Stagnation Flow with Arbitrary Surface Catalycity Including Low Reynolds Number Effects," *International Journal of Heat and Mass Transfer*, Vol. 9, No. 8, 1966, pp. 755–772.

[12]Cheng, H. K., and Chang, A. L., "Stagnation Region in Rarefied High Mach Number Flow," *AIAA Journal*, Vol. 1, No. 3, 1963, pp. 231–233.

Design Methodologies for Space Transportation Systems

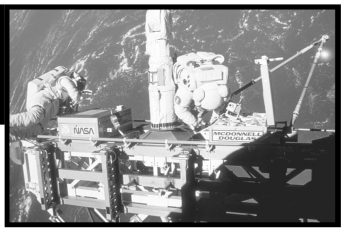

Walter E. Hammond

Design Methodologies for Space Transportation Systems is a sequel to the author's earlier text, *Space Transportation: A Systems Approach to Analysis and Design*. Reflecting a wealth of experience by the author, both texts represent the most comprehensive exposition of the existing knowledge and practice in the design and project management of space transportation systems. The text discusses new conceptual changes in the design philosophy away from multistage expendable vehicles to winged, reusable launch vehicles, and presents an overview of the systems engineering and vehicle design process as well as the trade-off analysis. Several chapters are devoted to specific disciplines such as aerodynamics, aerothermal analysis, structures, materials, propulsion, flight mechanics and trajectories, avionics, computers, and control systems. The final chapters deal with human factors, payload, launch and mission operations, and safety. The two texts by the author provide a valuable source of information for the space transportation community of designers, operators, and managers. A CD-ROM containing extensive software programs and tools supports the text.

Contents:
An Overview of the Systems Engineering and Vehicle Design Process ■ The Conceptual Design and Tradeoffs Process ■ Taking a Closer Look at the STS Design Sequence ■ Aerothermodynamics Discipline ■ Thermal Heating and Design ■ Structures and Materials ■ Propulsion Systems ■ Flight Mechanics and Trajectories ■ Avionics and Flight Controls ■ Multidisciplinary Design Optimization ■ Life Support and Human Factors/Ergonomics ■ Payloads and Integration ■ Launch and Mission Operations ■ Related Topics and Programmatics ■ Appendices

AIAA Education Series
Sept 2001, 839 pp, Hardcover ■ ISBN 1-56347-472-7
List Price: $94.95 ■ AIAA Member Price: $69.95 ■ Source: 945

AIAA
American Institute of Aeronautics and Astronautics

Publications Customer Service, P.O. Box 960, Herndon, VA 20172-0960
Fax: 703/661-1501 Phone: 800/682-2422 E-Mail: warehouse@aiaa.org
Order 24 hours a day at www.aiaa.org

01-0345